31st Annual International Conference of the IEEE EMBS
Minneapolis, Minnesota, USA, September 2-6, 2009

Optical Reflectance Spectroscopy for Detection of Human Prostate Cancer

Vikrant Sharma, Dheerendra Kashyap, Aditya Mathker, Sweta Narvenkar, Karim Bensalah, Wareef Kabbani, Altug Tuncel, Jeffrey A. Cadeddu, Hanli Liu

***Abstract*—We present the method and application of optical reflectance spectroscopy to differentiate prostate cancer from normal tissue using a needle like, bifurcated, fiber-optic probe. An analytical expression to model light reflectance recently published by Zonios et. al. was used to derive optical properties of tissue. A total of 23 cases of human prostate specimens were investigated to analyze statistical differences between the respective cancerous tissues versus normal tissues. The results demonstrate that the derived hemodynamic parameters and optical properties can serve as good bio-markers to differentiate tumor tissue from normal tissue in human prostate.**

I. Introduction

Optical techniques rely on spectral, angular and polarization characteristics of light scattered from the tissue; such characteristics can be used as biomarkers for specific medical applications. As an example, optical reflectance spectroscopy (ORS) has been utilized in various medical applications to identify tissue types [1], to diagnose diseased tissues [2], and to differentiate cancerous tissues from normal tissues [3-5]. In this case, tissue optical properties may themselves serve as biomarkers to differentiate cancerous lesions as light scattering and absorption are highly dependent on morphological and physiological state of the tissue.

Diffusion theory has been used to model the propagation of near-infrared (NIR) light in tissue. However, the diffusion approximation requires rigorous boundary conditions to be satisfied: (1) the source detector separation needs to be much larger than transport mean free path, and (2) the absorption coefficient, μ_a, needs to be much smaller than the reduced scattering coefficient, μ_s'. The diffusion approximation fails to model light propagation to be detected with a thin, needle-like probe since its source-detector separation (100 μm - 1 mm) is often of the similar order to the mean free path. In addition, the diffusion approximation could not be used for visible light since the magnitude of μ_a of hemoglobin in the visible light range is not necessarily much smaller than that of μ_s'. Although ORS has been investigated for its use in guiding minimally invasive surgeries and other clinical applications [1,2,6], it has been a challenge to derive a rigorous expression for a thin, needle-like reflectance probe to quantify tissue optical properties.

Recently, Zonios et. al. have developed an analytical expression for short source-detector separation measurements in tissue [7]. The model works in entire visible to NIR range and can be utilized for rapid monitoring of tissue physiology and morphology. However, very limited information on system calibration and model parameter determination is given in ref. [7]. In this paper, we present (1) rigorous calibration for two model parameters, k_1 and k_2, given in Zonios' model with limited known light scattering spectra, (2) utilization of a heuristic Ant Colony Optimization algorithm [8-9] to fit Zonio's model for quantifying hemodynamic parameters and μ_s' of tissue phantoms, and (3) the application of this methodology to detect prostate cancer using *ex vivo* human specimens.

Prostate cancer is the most common male cancer and second leading cause of death in men in the United States [10]. To improve prostate cancer diagnosis and treatment outcome, we are exploring the possibility of using ORS to detect prostate cancer in two specific areas: (1) ORS may allow to mark positive margins of cancer during prostatectomy in order to remove all the cancer margins, which are extended outside the prostate capsule but not visible to the naked eye. An optical probe that can differentiate between tumor tissue and various normal tissue types can provide a real-time solution for this problem. A recent publication [11] has reported such an approach in this direction. (2) We wish to explore that ORS may possibly be utilized to assist prostate cancer needle biopsy in the future since it is thin and can be possibly integrated with a biopsy needle.

For prostate adenocarcinoma (PA) diagnosis, we need first to examine whether the optical signatures are distinct between the cancerous tissue and benign tissue. Our recent study has proven that ORS has the ability to differentiate cancer features using a data-driven approach [12-14]. In the second part of this paper, we wish to report our model-based approach to analyze the measured ORS, which were taken

V. Sharma is with the International Techlink Group, Inc, Arlington, TX 76010 USA (evikrant@gmail.com);

D. Kashyap and A Mathker were with the Department of Bioengineering, University of Texas at Arlington, Arlington, TX 76019;

K. Bensalah and A. Tuncel were with the Department of Urology, University of Texas Southwestern Medical Center at Dallas, Dallas, TX 75390; W. Kabbani and J. A. Cadeddu are with the Department of Urology and Pathology, respetively, University of Texas Southwestern Medical Center at Dallas, Dallas, TX 75390

S. Narvenkar and H. Liu are with the Department of Biomedical Engineering, University of Texas at Arlington, Arlington, TX 76019 USA (phone: 817-272-2054; fax: 817-272-2251; e-mail: hanli@uta.edu).

from human prostate *ex vivo* specimens excised through laparoscopic surgery. The quantified hemoglobin concentrations and light scattering parameter, obtained using Zonios' model, are compared to see if they can serve as biomarkers to differentiate PA versus normal prostate tissue.

II. Materials and Methods

A. Analytical Model

The analytical model by Zonios et. al. relates the optical reflectance, $R_m(\lambda)$, measured with a short-distance optical probe, to the reduced scattering coefficient, $\mu_s'(\lambda)$, and absorption coefficient, $\mu_a(\lambda)$, of the medium, as given below:

$$R_m(\lambda) = \frac{\mu_s'(\lambda)}{k_1 + k_2\mu_a(\lambda)} \qquad (1)$$

where k_1 and k_2 are parameters depending on the geometrical characteristics of the measurement system, and for a set of probe and measurement system, they need to be calibrated using tissue phantoms. The spectral dependence of μ_a for blood-perfused tissues can be written as

$$\mu_a(\lambda) = [HbO]\,\varepsilon_{HbO}(\lambda) + [Hb]\,\varepsilon_{Hb}(\lambda) + \varepsilon_{H_2O}.\%H_2O \qquad (2)$$

where [*HbO*], [*Hb*] represent the concentrations of oxy- and deoxy- hemoglobin, respectively, λ is wavelength in nm, ε_x is extinction coefficient for chromophore *x*, and H_2O is the water content [15]. The spectral dependence of μ_s' can be approximated as given by Mie theory:

$$\mu_s = a.\lambda^{-b}, \quad \mu_s' = \mu_s(1-g), \quad g = 1.1 - (0.58\times10^{-3})\lambda \qquad (3)$$

where μ_s is the scattering coefficient, *g* is the anisotropic factor, *a* and *b* are both constants (a= 2.54x10^9, b=2.4, for 10% intralipid) and depend on the scatterer size and tissue type [16-17].

B. Instrumentation and Experimental Set Up

A CCD-array spectrometer (S2000, Ocean Optics, Dunedin, FL, USA), capable of collecting spectra in the range of 350-1050 nm, was used for diffuse reflectance measurements. However, measured spectra in the wavelength range of 500-850 nm were selected for data analysis. Light illumination was provided by a tungsten-halogen light source (HL2000HP, Ocean Optics, Dunedin, FL, USA). Two custom-built, thin fiber probes have been utilized in the study. Probe A was bifurcated with two 400-μm fibers, having an average separation of 800 μm between the two and a probe outer diameter of ~1.2 mm. The second probe, Probe B, was a 7-fiber-array probe (Ocean Optics, Dunedin, FL, USA), having a probe diameter of ~1.2 mm. Specifically, the 7 fibers in Probe B were arranged in a linear array across the center line, and channels 3 and 5 were used in this study. The diameter of each optical fiber in the array was ~100 μm. Two sets of constants k_1 and k_2 were determined for Probes A and B, respectively, by making measurements from liquid tissue-simulating phantoms made of animal blood and Intralipid solutions (Baxter Healthcare Corporation, Deerfield, IL). The effects of blood concentration, oxygenation, and Intralipid concentration on k_1 and k_2 were studied using Probe A, while the *in vivo* human specimen measurements were performed using Probe B. For calibration purpose, the measurements were also made with a dual-channel ISS Oximeter (ISS Inc., Champaign, IL), which is considered as the "gold standard" instrument and is often used to measure the values of μ_a and μ_s' from a sample solution.

C. Determination of k_1 and k_2 and Inverse Calculations

By reorganizing eq. (1), we get eq. (4)

$$\frac{\mu_s'(\lambda)}{R_m(\lambda)} = k_1 + k_2\mu_a(\lambda). \qquad (4)$$

This equation shows that k_1 and k_2 can be determined by obtaining a linear regression line that best fits $\mu_s'(\lambda)/R_m(\lambda)$ versus $\mu_a(\lambda)$. The ISS Oximeter can provide direct readings of μ_a and μ_s' values at two wavelengths (750 nm and 830 nm) as well as blood hemoglobin concentrations for the sample measured. We then converted the measured blood hemoglobin concentrations to the absorption coefficients in the visible and NIR range, $\mu_a(\lambda)$, by utilizing eq. (2). Similarly, the values of $\mu_s'(\lambda)$ in the visible and NIR region can be extrapolated/interpolated from the two μ_s' values at 750 nm and 830 nm using the Mie-theory based expression, eq. (3). These calculated values of μ_a and μ_s' were used along with $R_m(\lambda)$ to obtain k_1 and k_2.

After obtaining k_1 and k_2, it is possible to fit μ_a and μ_s' for a measured spectrum, $R_m(\lambda)$ based on eq. (1). The inverse calculation can be transformed into a problem of function minimization using an optimization algorithm. The algorithm searches for a set of values (e.g., chromophore concentrations and scattering parameters in this case) in the given solution space that best fit the measurement of ORS using least squares analysis. This process can be expressed as:

$$\chi^2 = \sum_{i=1}^{M}\left[R_m(\lambda_i)^{(measured)} - R_m(\lambda_i)^{(predicted)}\right]^2 \qquad (5)$$

where *M* is the number of wavelengths, $R_m(\lambda_i)^{(measured)}$ and $R_m(\lambda_i)^{(predicted)}$ are the reflectance values measured by the thin optical probe and calculated using eqs. (1) to (3) with the predicted values of [*Hb*], [*HbO*], and light scattering parameters, respectively, at wavelength λ_i. The water concentration was assumed to be constant at 80%. The Ant Colony Optimization algorithm, introduced by Marco Dorigo [8], is a probabilistic evolutionary technique for solving computational problems. This basic technique was modified in this study to suit function minimization.

In order to obtain optimal fit between the measured and calculated reflectance curve, we have incorporated multiple

iterations for optimization process. First, entire spectrum (500 nm – 845 nm) was used for curve fitting; the fitted values of [*Hb*], [*HbO*], *and* μ_s' were obtained. Second, the fitted μ_s' values were kept within 15% bounds, and the spectrum between 520 nm-590 nm was re-fitted to eqs. (1) to (3) for improved accuracy. This leads to optimal fitting for [*Hb*] and [*HbO*] since these chromophores exhibit strong spectral signatures between 520-590 nm. Third, [*Hb*] and [*HbO*] concentrations were fixed within 20% bounds while another re-fitting process took place using the entire spectrum again (500 nm -840 nm).

D. Tissue Phantoms and Human Prostate Specimens

In vitro tissue-simulating phantoms were prepared using stock Intralipid solutions and equine blood (Hemostat Inc, San Francisco, CA). The blood and intralipid were mixed and diluted with phosphate buffered saline (PBS) solution. Phantom experiments were conducted for determination of k_1 and k_2 as well as for validation of the inverse calculations. The phantoms were prepared with following combinations to test the algorithm: (1) with constant blood volume and intralipid volume, yeast was added to the solution in order to change absorption/oxygenation levels; (2) the blood concentration was kept constant while intralipid volume was changed in order to test the effect of change in scattering.

ORS readings of human prostate specimens were acquired at the University of Texas Southwestern Medical Center, Dallas, TX. All the measurements were taken in accordance with the guidelines set by the Institutional Review Board of University of Texas at Arlington and the University of Texas Southwestern Medical Center Dallas. The ORS data were collected from the prostate specimens *ex vivo* immediately after their resections through laparoscopic prostatectomy. A total of 23 cases of cancer-containing prostate specimens were investigated to derive statistical differences. Each prostate sample was bihalved so that the outside fibrous prostatic tissue and capsules were bypassed. The thin probe was then placed on various points on the tissue cross section, and data was acquired at each point. To be consistent across all the human specimens, we employed a standardized reference map for measurement locations (Fig. 1). After taking optical readings, the measured tissue locations were marked with a dye for further histology analysis, which serves as a gold standard to compare ORS readings.

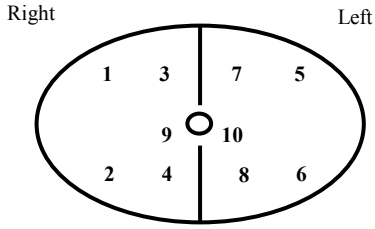

Fig. 1. Locations of ORS measurements on a cross section of bivalve prostate specimen. The central circle represents urethra; #1 to #8 indicates 8 measurement sites for each of the 23 human specimen.

III. Results

For Probe A, calibrated values of k_1 and k_2 were calculated while the hemoglobin oxygen saturation was varied from 20% -100%, resulting in k_1 = 16.04±0.19 cm^{-1} and k_2 = 3.77±0.05. The standard deviations indicate that the values remain unaltered as the optical properties of tissue phantoms are varied.

A. Inverse calculations and Algorithm Validation

In order to validate the method and algorithm, the inverse calculated values were compared with those obtained by the ISS Oximeter, which was used to provide good standard for absolute values of μ_a and μ_s'. Two types of phantom experiments were utilized. First, we fixed the scattering parameter of μ_s' with one concentration of Intrallipid and a total concentration of $[Hb_{Total}]$≅28 μM. We added 4 mg of yeast into the 3-liter phantom solution to alternate the oxygen saturation levels. Figures 2(a) shows a comparison between the calculated [*HbO*] and [*Hb*] versus those obtained from the ISS readings. Figures 2(c) shows the comparison of μ_s' and $[Hb_{Total}]$ along with the standard deviations. Secondly, Blood concentration was fixed at 34μM and intralipid volume was varied from 75-175 ml to obtain scattering changes. Figure 2(d) shows a comparison between the calculated values of μ_s' with ISS readings at 750 nm.

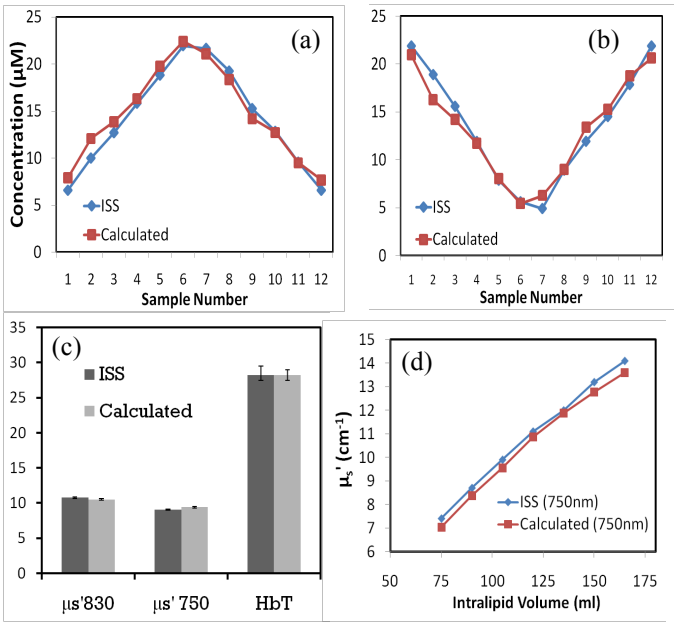

Fig. 2 Comparison of calculated values with the readings from the ISS oximeter, while blood oxygenation was varied. The figure shows (a) different [*HbO*] values, (b) different [*Hb*] values, (c) with μ_s' at 750 nm and 830 nm, as well as $[Hb_{Total}]$, averaged across 12 data points. (d) It shows μ_s' values with variation of Intralipid concentration.

B. Results from ex-vivo Prostate Specimen

In a similar way, probe B was calibrated and a set of k_1 and k_2 were obtained for its application. After we

obtained the spectral data from the *ex vivo* human prostate specimen, they were fitted using the reflectance model and the optimization algorithm, as described earlier. The values of [*Hb*], [*HbO*], [Hb_{total}], and μ_s' obtained were then grouped into cancer versus control. The average value of each of the parameters for the respective cases was calculated along with the Standard Deviation and the Standard Error. Besides a few outliners, most of the ORS spectra obtained (~200) have been used in the analysis, and the summarized results are shown in Fig. 3. This figure demonstrates the significant differences in [*HbO*], and [*Hb*] between control and cancerous prostate tissues in both cases. The important message learned is that the prostate cancerous tissue has enough intrinsic optical contrast to be differentiable from the control tissues.

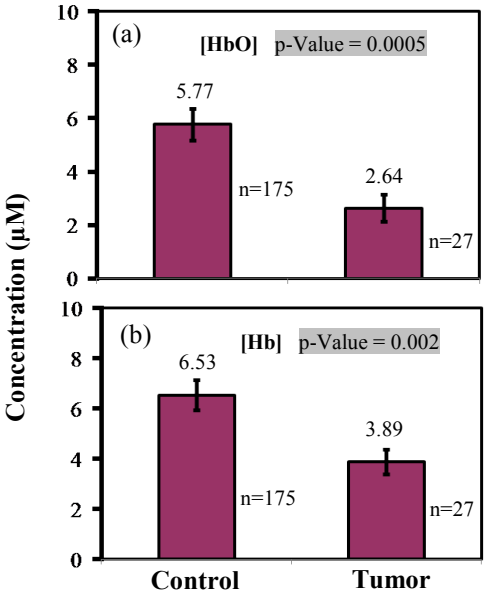

Fig. 3. It shows the differences in (a) [*HbO*] and (b) [*Hb*] between control and cancerous prostate tissues.

IV. Discussion and Conclusion

This study reported the rigorous calibration of a simple analytical model that describes diffuse reflectance at short source-detector separations taken from biological tissues. While this model is one of the simplest models as compared to other models, it relies greatly on two empirically determined parameters, k_1 and k_2. We showed that with different oxygen saturation levels set in the phantom, ranging from almost 10% to 90%, there was a minimal change in k_1 and k_2, thus proving that the parameters are not tissue dependent. We also simulated two scenarios where the (1) absorption and (2) scattering were changed independently. The calculated light scattering coefficient and hemodynamic parameters are in good agreement with the expected values given by the ISS Oximeter.

The calibrated set of k_1 and k_2 for Probe B were utilized for the measurements taken from the *ex vivo* human prostate specimens. A total of 23 cases of human prostate specimens were investigated, and the statistical differences between the cancerous tissues versus normal tissues were obtained. The results clearly demonstrate that the derived hemodynamic parameters can serve as good bio-markers to differentiate tumor tissue from normal tissue in human prostate.

References

[1] C. A. Giller, H. Liu, D.C. German, D. Kashyap, R.B. Dewey, "A stereotactic near-infrared probe for localization during functional neurosurgical procedures: further experience," *J. of Neurosurgery* **110**, 263–273 (2009).

[2] H. Radhakrishnan, Y. B. Peng, A.K. Senapati, D. Kashyap, and H. Liu, "Light scattering from rat spinal cord and sciatic nerves measured *in vivo* by near infrared reflectance spectroscopy," *J. of Biomed. Opt.* **10**(5), 051405(1-8) (2005).

[3] U. Utzinger, M. Brewer, E. Silva, D. Gershenson, R.C. Blast, Jr., M. Follen, and R. Richards-Kortum, "Reflectance Spectroscopy for In Vivo Characterization of Ovarian Tissue," *Lasers in Surgery and Medicine* **28**, 56–66 (2001).

[4] L. T. Perelman, V. Backman, M. Wallace, G. Zonios, R. Manoharan, A. Nusrat, S. Shields, M. Seiler, C. Lima, T. Hamano, I. Itzkan, J. Can Dam, J.M. Crawford, and M.S. Feld, "Observation of periodic fine structure in reflectance from biological tissue: a new technique for measuring nuclear size distribution," *Phys. Rev. Lett.* **80**, 627-630 (1998).

[5] I. J. Bigio, S. G. Bown, G. Briggs, C. Kelley, S. Lakhani, D. Pickard, P. Ripley, I. G. Rose, and C. Saunders, "Diagnosis of breast cancer using elastic-scattering spectroscopy: preliminary clinical results," *J. Biomed. Opt.* **5**, 221-228 (2000).

[6] C. A. Giller, H. Liu, P. Gurnani, S. Victor, U. Yazdani, D. C. German, "Validation of a near-infrared probe for detection of thin intracranial white matter structures," *J. Neurosurg.* **98**, 1299-1306 (2003).

[7] G. Zonios and A. Dimou, "Modeling diffuse reflectance from semi-infinite turbid media: application to the study of skin optical properties," *Opt. Express* **14**, 8661-8674 (2006).

[8] M. Dorigo and L. M. Gambardella, "Ant Colony System: A cooperative learning approach to the travelling salesman problem," *IEEE Trans. Evol. Comp.* **1**, 53-66 (1997).

[9] B. P. Wang and A. Apte, "Design optimization using ant colony system," presented at *Chinese Society for Mechanical Engineers*, Taipei, Taiwan, 2003.

[10] S. H. Landis, T. Murray, S. Bolden, et al. "Cancer Statistics 1999.CA", *Cancer J Clin* 9: 8-13 (1999).

[11] G. Salomon, T. Hess, A. Erbersdobler, C. Eichelberg, S. Greschner, A. N. Sobchuk, A. K. Korolik, N. A. Nemkovich, J. Schreiber, M. Herms, M. Graefen, H. Huland, "The Feasibility of Prostate Cancer Detection by Triple Spectroscopy," *European Urology* **55**, 376–384 (2009).

[12] K. Bensalah, A. Tuncel, D. Peshwani, I. Zeltser, H. Liu, and J.A. Cadeddu, "Optical reflectance spectroscopy to differentiate renal tumor from normal parenchyma," *J. of Urology* 179(5), 2010-2013 (2008).

[13] K. Bensalah, D. Peswani, A. Tuncel, J.D. Raman, I. Zeltser, H. Liu and J.A. Cadeddu, "Optical Reflectance Spectroscopy to Differentiate Benign and from Malignant Renal Tumors at Surgery," *J. of Urology* 73(1), 178-181 (2009).

[14] S.B. Kim, C. Temiyasathit, K. Bensalah, A. Tuncel, J. Cadeddu, W. Kabbani, A.V. Mathker, and H. Liu, "An efficient procedure for classification of prostate cancer in optical spectra," submitted to Expert Systems with Applications, 2009.

[15] S. J. Matcher, M. Cope and D. T. Delpy, "Use of the water absorption spectrum to quantify tissue chromophore concentration changes in near-infrared spectroscopy," *Phys. Med. Biol.* **39**, 177-196 (1994).

[16] Hugo J. van Staveren, Christian J. M. Moes, Jan van Marie, Scott A. Prahl, and Martin J. C. van Gemert, "Light scattering in Intralipid-10% in the wavelength range of 400–1100 nm," *Appl. Opt.* **30**, 4507-4514 (1991).

[17] S. Jacques, Oregon Medical Laser Center, April "Optical properties of "IntralipidTM", an aqueous suspension of lipid droplets", "*http://omlc.ogi.edu/spectra/intralipid/index.html"*